The Spectrum
of the Discrete Quantum Pendulum

B C. Kreft[1]

Technische Universität Berlin, Fachbereich Mathematik,
MA 7-2, Straße des 17.Juni 132, D-10623 Berlin,
e-mail: kreft@math.tu-berlin.de

December 31 , 1993
revised Mai 3, 1994

SFB 288 Preprint No. 80 B

B

Abstract

A In this paper we study spectral properties of the Quantum Pendulum Model by analytical and numerical methods. We derive a Chamber's relation, study the parameter dependency of the band spectrum and chernnumbers, perform a semiclassical analysis, compute the Husimi transfomation of the eigenfunctions and the density of states for some parameter values. The numerical analysis of this model reveals a relation between short spectral bands, large gaps, localized states and small chernnumber on one hand and long bands, small gaps, extended states and large chernnumber on the other hand.

---

[1] This work was supported by the Deutsche Forschungsgemeinschaft,
:q! Sonderforschungsbereich 288 "Differentialgeometrie und Quantenphysik"

1 Introduction

In solid state physics the energy spectrum of electrons in a periodic lattice potential is changed drastically by a uniform magnetic field. Assuming non-interacting electrons and separating the problem in directions parallel and perpendicular to the field leads to the study of 2D-Bloch electrons in a constant magnetic field.

For a square lattice with nearest-neighbour hopping interaction the Hofstadter model described by Harper's equation belongs to this class of problems. It has been analysed by physicists and mathematicians for many years.

In this paper we study a new family of models, the so-called doubly-discrete Quantum Pendulum. It has been introduced by Bobenko, Kutz and Pinkall [6] in the study of the doubly discrete sine-Gordon equation. We analyse its spectral properties and compute both the spectrum and the eigenfunctions numerically.

In order to do so we especially use the algebraic framework from [10], [4] and the semiclassical methods from [13]-[15], [26].

In the algebraic setting we consider the Rotational algebra $\mathcal{A}_\Phi$ generated by the unitary magnetic translation operators T_1 and T_2 in the lattice unit directions on $l^2(\mathbf{Z}^2)$.

$$\begin{aligned} T_1 f(r,s) &= f(r+1,s) && (1)\\ T_2 f(r,s) &= e^{i\Phi r} f(r,s+1)\,. && (2)\end{aligned}$$

The fundamental commutation relation is

$$T_1 T_2 = T_2 T_1 e^{i\Phi}\,. \tag{3}$$

$\Phi \in [0, 2\pi]$ is the magnetic flux per lattice unit-cell.

The Hofstadter Hamiltonian H_{Hof} is element of $\mathcal{A}_\Phi$ and given by

$$H_{\mathrm{Hof}} = T_1 + T_2 + T_1^\star + T_2^\star \tag{4}$$

Physically, the four terms of H_{Hof} describe the hopping interactions with the four direct neighbours in a square lattice. (Fig. 1 a))

Other models, like the triangular lattice [5] or the second neighbour model [3], are given by other self-adjoint polynomials in T_1 and T_2. In this paper we study a special case of the next-nearest-neighbour (NNN) model [12] defined by the Hamiltonian

$$H = \epsilon(T_1 + T_2 + T_1^\star + T_2^\star) + k\left(e^{-i\frac{\Phi}{2}} T_1 T_2 + e^{i\frac{\Phi}{2}} T_2^\star T_1^\star\right) + \frac{1}{k}\left(e^{i\frac{\Phi}{2}} T_1 T_2^\star + e^{-i\frac{\Phi}{2}} T_2 T_1^\star\right) \tag{5}$$

Using the Weyl operator

$$T(m) := e^{i\Phi/2 m_1 m_2} T_1^{m_2} T_2^{-m_1} \qquad \left(m = (m_1, m_2) \in \mathbf{Z}^2\right)$$

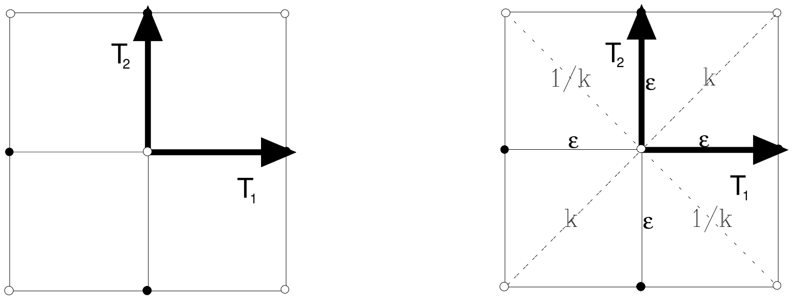

a) b)

Figure 1: Nearest-neighbour interaction in lattice models : a) Hofstadter , b) Quantum Pendulum

it is rewritten as

$$H = \epsilon (T(1,0) + T(-1,0)) + kT(-1,1) + \frac{1}{k} T(1,1) + \text{h.c.}\ .$$

The model describes the hopping to all eight neighbours in a square lattice with an anisotropic choice of the interaction strength (Fig. 1 b)).

In the semi-classical picture we consider the canonical position and momentum operators $\hat{x}$ and $\hat{p}$. If we replace in the Heisenberg relation Planck's constant by the magnetic flux Φ we get a representation of the fundamental commutation relation (3) by

$$T_1 = e^{i\hat{x}}, \quad T_2 = e^{i\hat{p}}, \quad [\hat{x}, \hat{p}] = i\Phi. \tag{6}$$

In the semi-classical limit, obtained for $\Phi \longrightarrow 0$, the operators $\hat{x}, \hat{p}$ turn into into the classical position and momentum coordinates x, p . Thus the Hofstadter Model has the classical symbol

$$H_{\text{Hof}}(p, x) = 2\cos(x) + 2\cos(p). \tag{7}$$

For the Quantum Pendulum we have

$$H(p, x) = 2\epsilon (\cos(x) + \cos(p)) + 2k \cos(x + p) + \frac{2}{k} \cos(x - p). \tag{8}$$

Note that both symbols (7) and (8) are periodic in x and in p.

From the contour levels in classical phase space it becomes obvious why the model is called Pendulum. In each unit cell of the phase space picture (Fig. 2) we have closed orbits at small energies. They are related to oscillating solutions. At high energies we see extended contours giving rise to rotating solutions.

The parameter k is the analog of the gravitational constant in the usual pendulum and controls the onset of rotating solutions. The parameter ϵ switches between Hofstadter Model ($\epsilon = 0$) and Pendulum behavior ($\epsilon \neq 0$) as we will show later.

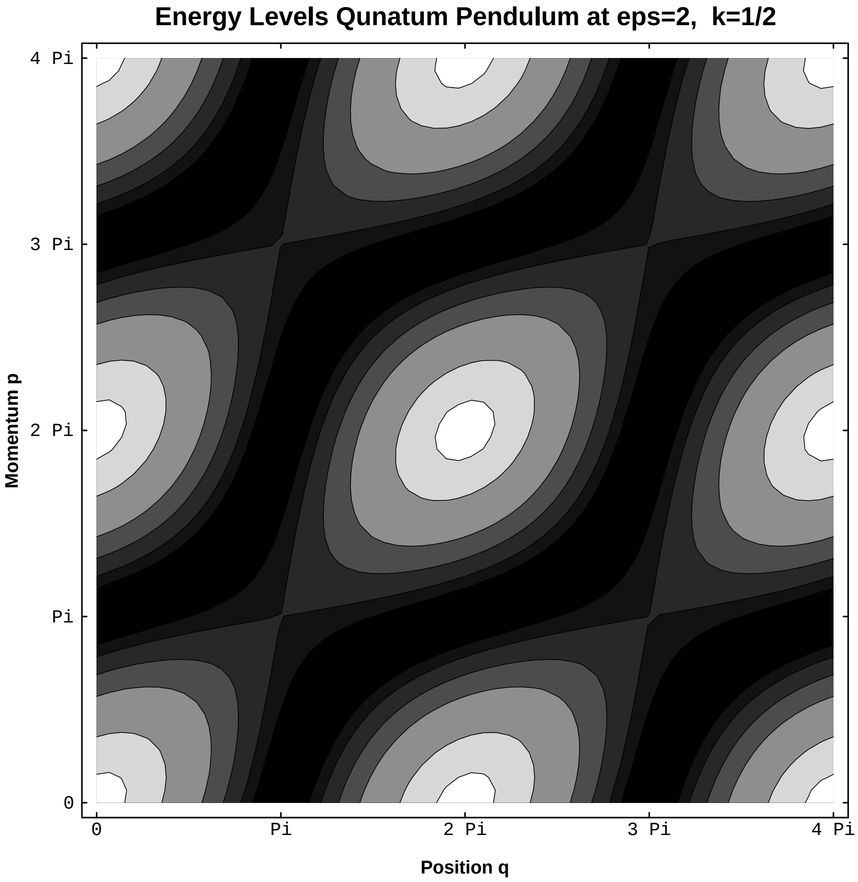

Figure 2: Classical Energy Contours of Quantum Pendulum at $\epsilon = 2$, $k = \frac{1}{2}$

In this paper we study the spectral properties of the discrete Quantum Pendulum for rational flux $\Phi = 2\pi\frac{p}{q}$.

The spectrum of the Quantum Pendulum model exhibits many symmetries, which can, in the algebraic framework, be identified with algebra-automorphisms of the Rotational Algebra. They are studied in Section 2. On the semi-classical level the symmetries are related to transformations of the classical phase space. In certain limits of ϵ and k the Quantum Pendulum model is related to various other Hofstadter-like models (triangular lattice, square lattice and free discrete Laplace). The symmetries allows one to restrict the parameter space to the strip $(\epsilon, k) \in \mathbf{R}_+ \times (0,1]$ for further studies.

In Section 3 we introduce, via Bloch analysis, the matrix representation for the Rotational Algebra $\mathcal{A}_\Phi$ with rational flux $\Phi = 2\pi\frac{p}{q}$.

An analog of Chamber's relation is derived in Section 4. It shows that, as in the Hofstadter model, the characteristic polynomial for the Quantum Pendulum matrix at rational flux decomposes into a polynomial of degree q, independent of the Bloch vector, and an offset function, independent of the energy. The offset function is a rescaled version of the classical symbol $H(p,x)$. We can determine the band edges of the Hamiltonian $H(\epsilon,k)$, by studying the critical points of the classical symbol $H(x,p)$, as it is done in Section 5. This leads to the numerical computation of the spectrum for different values of the parameters ϵ and k in Section 6.

The spectrum shows a nesting structure like other models of the Hofstadter type, too. Moreover the Pendulum behavior in our model produces two different energy regimes in the spectrum. For small energies we see long bands and very small gaps. In the semi-classical limit they are related to classically rotating solutions. For high energies we have short bands and large gaps in the spectrum, which is typical for energies at classically oscillating solutions.

We compute the semi-classical expansion for the spectrum in the oscillating regime in Section 7. It shows a good agreement with the matrix spectra even for large values of the semi-classical parameter Φ.

Finally in Section 8 we study the eigenstates for energies with both rotating and oscillating solutions, the localization of the Husimi transformation of the eigenstates, the chernnumbers and the density of states.

It is found that the Husimi transformation of the eigenstates is localized in the vicinity of the classical trajectories. Classically rotating solutions belong to extended states and the Chernnumbers for the related spectral bands have a large absolute value. Conversely, classically oscillating solutions generate localized quantum states with a small absolute value of the Chernnumbers.

2 Symmetries of $H(\epsilon, k, \Phi)$

Before carrying out the computation of the spectrum we analyze the parameter dependency of the Hamiltonian $H(\epsilon, k, \Phi)$. Due to symmetries it is sufficient to restrict further studies to the strip $\epsilon \geq 0,\ k \in (0,1]$ and to fluxes $\Phi \in [0, 2\pi]$. Certain limits in the parameters ϵ and k of our model lead to the Hofstadter Model, the triangular lattice and the Mathieu-Hamiltonian.

Let us denote the spectrum of $H(\epsilon, k, \Phi)$ by $\sigma(\epsilon, k, \Phi)$. If some parameter is not involved in a symmetry it will be omitted.

In this Hofstadter-like models we can prove symmetries very efficiently using the algeraic framework by considering homomorphisms of the Rotational Algebra. We will demonstrate this method by an example.

Proposition 1

$$\sigma(k) = \sigma(1/k)$$

Proof : Consider the algebra homomorphism $\pi : \mathcal{A}_\Phi \mapsto \mathcal{A}_\Phi$ generated by

$$\pi(T_1) = T_2, \quad \pi(T_2) = T_1^\star$$

Then

$$\pi\left(H(k)\right) = H(1/k)$$

Since π does not change the spectrum Proposition 1 is proved. $\square$

Most of the symmetries have an interpretation in the classical phase space picture, too. E.g. the above example is related to a rotation of the phase space by $\pi/2 : x \rightarrow p, p \rightarrow -x$.

In Table 1 we list other symmetries of the Quantum Pendulum. Where it exists we give the algebra homomorphism and the classical phase space transformation, too. The last three relations in the table are either purely algebraic or derived from the first cases.

Thus in the following discussions we can restrict the parameter space to the strip

$$\epsilon \geq 0,\ k \in (0,1]\,,\ \Phi \in [0, 2\pi)\,.$$

At the end of this Section we consider some limit cases of the discrete Quantum Pendulum.

Setting $\epsilon = 0$ gives a Mathieu Hamiltonian with rescaled energy $\tilde{E} = kE$ and doubled flux $\tilde{\Phi} = 2\Phi$

$$\begin{aligned} H\left(\epsilon = 0\right) &= k\left(e^{i\frac{\Phi}{2}} T_1 T_2 + e^{-i\frac{\Phi}{2}} T_2^\star T_1^\star\right) + \frac{1}{k}\left(e^{i\frac{\Phi}{2}} T_1 T_2^\star + e^{-i\frac{\Phi}{2}} T_2 T_1^\star\right) \\ &= k\left(\tilde{T}_1 + \tilde{T}_1^\star + \frac{1}{k^2}\left(\tilde{T}_2 + \tilde{T}_2^\star\right)\right). \end{aligned}$$

spectral symmetry	:	$\sigma(k) = \sigma(1/k)$
algebraic picture	:	$T_1 \to T_2$,
		$T_2 \to T_1^\star$
classical picture	:	$x \to p$,
		$p \to -x$
		rotation by $\pi/2$
spectral symmetry	:	$\sigma(\epsilon) = \sigma(-\epsilon)$
algebraic picture	:	$T_1 \to -T_1$,
		$T_2 \to -T_2$
classical picture	:	$x \to -x$,
		$p \to -p$
		reflection at the origin
spectral symmetry	:	$\sigma(\Phi) = \sigma(-\Phi)$
algebraic picture	:	$T_1 \to T_2$,
		$T_2 \to T_1$,
		$\mathcal{A}_\Phi \to \mathcal{A}_{-\Phi}$
classical picture	:	$x \to p$,
		$p \to x$
		reflection at line $x = p$
spectral symmetry	:	$\sigma(\epsilon, k) = -\sigma(-\epsilon, -k)$
algebraic picture	:	$H(\epsilon, k) = -H(-\epsilon, -k)$
classical picture	:	same
		reverse sign of energy scale
spectral symmetry	:	$\sigma(\Phi) = -\sigma(\Phi + 2\pi)$
algebraic picture	:	$H(\Phi, k) = H(\Phi + 2\pi, -k)$, and $\sigma(k) = -\sigma(-k)$
		$\mathcal{A}_\Phi = \mathcal{A}_{\Phi+2\pi}$
classical picture	:	no classical interpretation
spectral symmetry	:	$\sigma(k) = -\sigma(-k)$
derived by	:	$\sigma(\epsilon, k) = -\sigma(-\epsilon, k) = -\sigma(\epsilon, k)$

Table 1: Symmetries of the Quantum Pendulum

Here we used the algebra homomorphism [22] given by

$$\begin{aligned}\tilde{\Phi} &= 2\Phi\,,\\ \tilde{T}_1 &= e^{i\frac{\Phi}{2}}T_2^\star T_1^\star,\\ \tilde{T}_2 &= e^{i\frac{\Phi}{2}}T_1 T_2^\star.\end{aligned}$$

For $k = 1$ we get the Hofstadter Hamiltonian with doubled flux $\tilde{\Phi} = 2\Phi$.

For $\epsilon \to \infty$ and $k \approx 1$ the Quantum Pendulum Model is dominated by the first four terms. Thus we get a perturbed Hofstadter Hamiltonian with rescaled energy, but flux Φ.

For $k \to 0$ the term with $\frac{1}{k}$ dominates the Hamiltonian and the system resembles the discrete Laplace operator

$$\begin{aligned}H &\to \frac{1}{k}\left(e^{i\frac{\Phi}{2}}T_1T_2^\star + e^{-i\frac{\Phi}{2}}T_2T_1^\star\right)\\ &= \frac{1}{k}\left(\tilde{T}_2 + \tilde{T}_2^\star\right)\end{aligned}$$

with spectrum $[-2\frac{1}{k}, 2\frac{1}{k}]$.

Finally, if $\epsilon = k$, the Hamiltonian is related to a triangular lattice model with rescaled energy.

$$\begin{aligned}H &= \epsilon\left(T_1 + T_2 + T_1^\star + T_2^\star + e^{i\frac{\Phi}{2}}T_1T_2 + e^{-i\frac{\Phi}{2}}T_2^\star T_1^\star\right)\\ &\quad + \frac{1}{\epsilon}\left(e^{i\frac{\Phi}{2}}T_1T_2^\star + e^{-i\frac{\Phi}{2}}T_2T_1^\star\right)\\ &= \epsilon\left(H_{\text{triangle}}\right) + \frac{1}{\epsilon}\left(e^{i\frac{\Phi}{2}}T_1T_2^\star + e^{-i\frac{\Phi}{2}}T_2T_1^\star\right).\end{aligned}$$

In the next Sections we show how to reduce the computation of the spectrum for rational flux to a matrix problem by using Bloch analysis.

3 Rational Flux and Matrix Representation

For rational flux $\Phi = 2\pi\frac{p}{q}$ with $p, q \in \mathbf{Z}$ relative prime the magnetic translations T_1 and T_2^q generate a commuting subgroup in $\mathcal{A}_\Phi$. We can apply Bloch's theorem and get a direct integral decomposition of the Hilbert space $l^2(\mathbf{Z}^2) = \int_{\mathbf{B}}^{\oplus} d^2\theta\, \mathcal{H}(\theta)$ over fibers $\mathcal{H}(\theta) = \mathbf{C}^q$ and Brillouin zone $\mathbf{B} = [0, 2\pi]^2$. (This decomposition is analogous to the continuous case as it is shown in e.g. [23].)

The generators T_1 and T_2 decompose into

$$T_j(\theta) = e^{i\theta_j} W_j \qquad (\theta = (\theta_1, \theta_2) \in \mathbf{B},\ j = 1, 2)$$

where W_1 is the cyclic permutation on $\mathbf{C}^q$ and W_2 is a diagonal matrix.

$$W_1 = \begin{pmatrix} 0 & 1 & 0 & 0 \\ & \ddots & \ddots & 0 \\ & & \ddots & 1 \\ 1 & & & 0 \end{pmatrix}, \quad W_2 = \operatorname{diag}\left(e^{i\Phi}, e^{i2\Phi}, \ldots, e^{iq\Phi}\right).$$

Again W_1 and W_2 fulfill the fundamental commutation relation 3

$$W_1 W_2 = W_2 W_1 e^{i\Phi}.$$

Note that

$$W_1^q = W_2^q = \mathbf{1} \quad \text{and} \quad \det(W_1) = \det(W_2) = (-1)^{q-1}.$$

In each fiber $\theta = (\theta_1, \theta_2)$ the Hamiltonian has the form

$$H(\theta) = \begin{pmatrix} a_1 & b_1 & 0 & \cdots & \bar{b}_q \\ \bar{b}_1 & a_2 & b_2 & & \\ 0 & \bar{b}_2 & a_3 & \ddots & 0 \\ \vdots & & \ddots & \ddots & b_{q-1} \\ b_q & & 0 & \bar{b}_{q-1} & a_q \end{pmatrix} \tag{9}$$

with

$$\begin{aligned} a_l(\theta) &= 2\epsilon \cos(\Phi l + \theta_2) \\ b_l(\theta) &= \epsilon e^{i\theta_1} + k e^{i\theta_1 + i\theta_2 + i\Phi\left(l + \frac{1}{2}\right)} + \frac{1}{k} e^{i\theta_1 - i\theta_2 - i\Phi\left(l + \frac{1}{2}\right)}. \end{aligned}$$

and $l = 1, 2, \ldots q$.

Rewriting the eigenvalue equation for each fiber

$$H(\theta)\vec{\psi} = E(\theta)\vec{\psi}, \quad (\vec{\psi} \in \mathbf{C}^q)$$

in terms of q-periodic sequences $\psi(l) := \vec{\psi}_{l \bmod q}$, ($l \in \mathbf{Z}$), we obtain the analog of Harper's equation for the discrete Quantum Pendulum

$$a_l(\theta)\psi(l) + b_l(\theta)\psi(l+1) + \bar{b}_{l-1}(\theta)\psi(l-1) = E(\theta)\psi(l).$$

For fixed θ we have q eigenvalues, defining the band functions

$$E_1(\theta) \leq E_2(\theta) \leq E_3(\theta) \leq \cdots \leq E_q(\theta)$$

which are continous in θ.

The spectrum of H is the union of the spectra of $H(\theta)$ over all fibers [23]

$$\mathrm{spec}(H) = \overline{\bigcup_{\theta \in \mathbf{B}} \mathrm{spec} H(\theta)} = \bigcup_{l=1,\cdots q,\, \theta \in \mathbf{B}} \mathrm{Range}\left(E_l(\theta)\right).$$

The computation of $\mathrm{Range}\left(E_l\right) = \left[E_l\left(\theta^{(l)}_{\mathrm{min}}\right), E_l\left(\theta^{(l)}_{\mathrm{max}}\right)\right]$ is simple, if we know the critical points $\theta^{(l)}_{\mathrm{min}}$, $\theta^{(l)}_{\mathrm{max}}$ where the band functions take their minimum and maximum.

For our model these points can be computed explicitely using an analog of Chamber's relation for the Harper equation. The latter shall be drrived in the next Section.

4 The Secular Determinant

Chamber's relation for the Hofstadter model states that the secular determinant of $H(\theta)$ has the form

$$\det\left(H(\theta)-z\mathbf{1}\right)=p(z)-h(\theta).$$

$p(z)=(-z)^q+\ldots$ is a polynomial of degree q independent of θ and $h(\theta)=2\cos(q\theta_1)+2\cos(q\theta_2)$ is independent of z. For our model the same type of relation holds. A general result of this form for the NNN-model has been shown in [12]. For the Quantum Pendulum the offset-function $h(\theta)$ reveals a rather simple form involving Chebyshev polynomials.

To demonstrate the technique and to derive a helpful result let us first examine the following diagonal operator

$$A=kT_2+\frac{1}{k}T_2^\star$$

In the matrix representation A reads

$$A(\theta)=ke^{i\theta}W_2+\frac{1}{k}e^{-i\theta}W_2^\star,\quad (\theta\in[0,2\pi]).$$

It is unitarily equivalent to $ke^{i\theta}W_1+\frac{1}{k}e^{-i\theta}W_1^\star$. For $k=1$ this is the discrete Laplacian on $\mathbf{C}^q$.

Proposition 2 *The secular determinant of $A(\theta)$ is*

$$\det\left(A(\theta)-z\mathbf{1}\right)=(-1)^q 2\,P_q\left(\frac{z}{2}\right)+(-1)^{q-1}\left(k^q e^{i\theta q}+\frac{1}{k^q}e^{-i\theta q}\right).$$

where $P_n(x)=\cos\left(n\arccos(x)\right)$ is the n-th Chebyshev polynomial.

Proof: From the commutation relation (3) we get

$$W_1\,W_2W_1^{-1}=e^{i\Phi}W_2.$$

Since p and q have no common divisor we can, by Euklid's Theorem, find numbers $l,m\in\mathbf{Z}$ such that $lp-qm=1$ and

$$\Phi l=2\pi\frac{pl}{q}=2\pi\frac{1}{q}+2\pi m.$$

Thus $A(\theta)$ is unitarily equivalent to $A(\theta+\frac{2\pi}{q}m)$, $(m\in\mathbf{Z}^2)$ and $\det\left(A(\theta)-z\mathbf{1}\right)$ is $\frac{2\pi}{q}$ -periodic. Expanding the secular determinant in a Fourier series and defining $\zeta=e^{i\theta}$ we have

$$\det\left(k\zeta W_2+\frac{1}{k}\zeta^{-1}W_2^\star-z\mathbf{1}\right)=b(z)+\zeta^q b_1(z)+\zeta^{-q}b_2(z).\tag{10}$$

On the right side we have not written explicitly the k dependency of each of the terms. The series has no terms of order higher than ζ^q, since the determinant is a polynomial of order q in its coefficient. Dividing equation (10) by ζ^q and taking the limit $\zeta \to \infty$ gives :

$$b_1(z) = \det(kW_2) = k^q(-1)^{q-1}.$$

Analogously we find $b_2(z) = \frac{1}{k^q}(-1)^{q-1}$. Thus Chamber's formula for $A(\theta)$ is

$$\det\left(A(\theta) - z\mathbf{1}\right) = b(z) + (-1)^{q-1}\left(k^q e^{i\theta q} + \frac{1}{k^q}e^{-i\theta q}\right). \tag{11}$$

On the other hand, since $A(\theta)$ is diagonal

$$\det\left(A(\theta) - z\mathbf{1}\right) = \prod_{l=1}^{q}\left(ke^{i\Phi l}\zeta^{-1} + \frac{1}{k}e^{-i\Phi l}\zeta - z\right). \tag{12}$$

Choosing $\zeta_0 = ke^{i\theta_0}$, $\theta_0 = \arccos(z/2)$ the r.h.s of (12) vanishes. Together with (11) we get

$$\begin{aligned} \det\left(A(\theta_0) - z\mathbf{1}\right) &= 0 \\ &= b(z) + (-1)^{q-1}\left(k^q\zeta_0^q + \frac{1}{k^q}\zeta_0^{-q}\right) \\ &= b(z) + (-1)^{q-1}\left(2\cos(q\theta_0)\right) \\ &= b(z) + (-1)^{q-1}\left(2\cos(q\arccos(z/2))\right). \quad \Box \end{aligned}$$

Chamber's relation for the discrete Quantum Pendulum is now given by

Proposition 3 *The secular determinant for the discrete Quantum Pendulum (9) is*

$$\det\left(H(\theta) - z\mathbf{1}\right) = p(z) + h(\theta)$$

where $p(z) = (-z)^q + \ldots$ *is a Polynomial of degree* q*,*

$$\begin{aligned} h(\theta_1, \theta_2) &= -4P_q(-\epsilon/2)\left[\cos(q\theta_1) + \cos(q\theta_2)\right] + \\ &\quad 2(-1)^p\left[k^q\cos\left(q(\theta_1+\theta_2)\right) + \frac{1}{k^q}\cos\left(q(\theta_1-\theta_2)\right)\right] \end{aligned}$$

and $P_n(x)$ *is the* n*-th Chebyshev polynomial.*

Proof : Again because of (3)

$$W_1^{m_2}W_2^{-m_1}H(\theta)W_2^{m_1}W_1^{-m_2} = H(\theta + \Phi m), \quad (m_1, m_2) \in \mathbf{Z}$$

and the secular determinant $\det(H(\theta) - z\mathbf{1})$ is periodic in θ_1 and θ_2 with period $2\pi/q$.

It can be written as a Fourier series in $\zeta_j^q = \exp(iq\theta_j)\,(j=1,2)$.

$$\begin{aligned}
\det\left(H(\theta) - z\mathbf{1}\right) &= \\
&= \det\Big(\epsilon\left(W_1\zeta_1 + W_2\zeta_2 + W_1^{-1}\zeta_1^{-1} + W_2^{-1}\zeta_2^{-1}\right) \\
&\quad + e^{i\frac{\Phi}{2}}\left(\frac{1}{k}W_1W_2^\star\zeta_1\zeta_2^{-1} + kW_2^\star W_1^\star\zeta_1^{-1}\zeta_2^{-1}\right) \\
&\quad + e^{-i\frac{\Phi}{2}}\left(\frac{1}{k}W_2W_1^\star\zeta_1^{-1}\zeta_2 + kW_1W_2\zeta_1\zeta_2\right) - z\mathbf{1}\Big) \qquad (13) \\
&= \sum_{|n_1|,|n_2|\le 1} a_n(z)\zeta_1^{qn_1}\zeta_2^{qn_2} \qquad (14)
\end{aligned}$$

Dividing equation (13) by ζ_1^q and taking the limit $\zeta_1^q \to \infty$

$$\begin{aligned}
& a_{(1,0)}(z) + a_{(1,1)}(z)\zeta_2^q + a_{(1,-1)}(z)\zeta_2^{-q} \\
=\ & \det(W_1)\det\left(\epsilon\mathbf{1} + e^{i\frac{\Phi}{2}}\frac{1}{k}\zeta_2^{-1}W_2^\star + e^{-i\frac{\Phi}{2}}\frac{1}{k}\zeta_2W_2\right) \\
=\ & \det(W_1)\det\left(A(\theta_2 - \frac{\Phi}{2}) - (-\epsilon)\right) \qquad (15)
\end{aligned}$$

Dividing by ζ_2^q, the limit $\zeta_2 \to \infty$ gives

$$a_{(1,1)} = \det(W_1)\det(ke^{-i\frac{\Phi}{2}}W_2) = k^q\exp(\frac{\Phi}{2}q) = (-1)^p$$

Analogously we find $a_{(1,-1)} = (-1)^p\frac{1}{k^q}$. Inserting this results into (15) and using proposition (2) finishes the proof. □

The derivative of the eigenvalue equation $p\left(E(\theta)\right) + h(\theta) = 0$

$$p'\left(E(\theta)\right)\,\nabla E(\theta) = -\nabla h(\theta)$$

shows that critical points of $h(\theta)$ are critical points of $E(\theta)$, too, provided we have no band touching : $p'\left(E(\theta)\right) \neq 0$.

Thus the spectrum of H is the inverse image of $Range(h(\theta))$ under the polynomial $p(z)$. This connection is visualized in Fig. 3. The solid line is the graph of $p(z)$ and the dotted lines denote the range of $h(\theta)$. An energy value z on the x-axis belongs to the spectrum if the graph of the polynomial $p(z)$ at this energy lies between the dotted lines.

Note that $h(\theta)$ has the same form as the classical symbol $H(x,p)$ with the replacement $x \to q\theta_1$, $p \to q\theta_2$, $k \to (-1)^p k^q$ and $\epsilon \to -2P_q(-\epsilon/2)$.

Thus to find the band edges it is sufficient to discuss the critical points of the classical symbol. The result of this analysis is presented in the next Section.

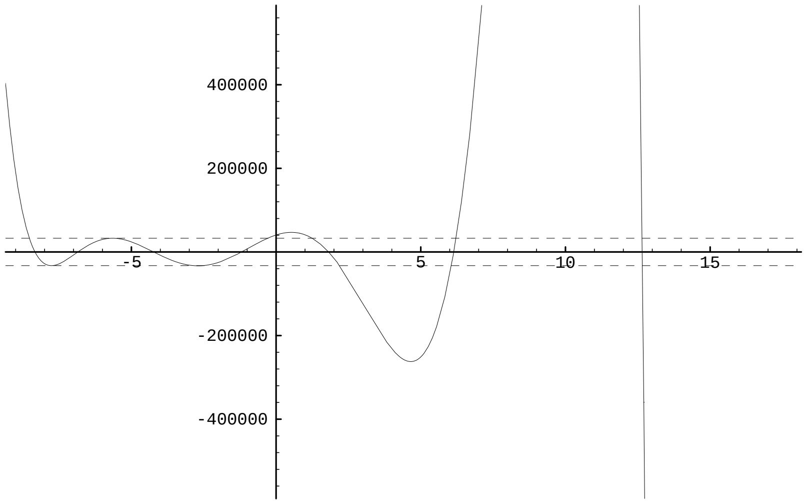

Figure 3: Characteristic Polynomial for $\epsilon = 2$, $k = 1/4$, $p = 1$, $q = 7$

5 Discussion of the Classical Symbol

The classical symbol

$$H(p, x) = 2\epsilon\left(\cos(x) + \cos(p)\right) + 2k\cos(x + p) + \frac{2}{k}\cos(x - p). \tag{16}$$

of the Quantum Pendulum is periodic in position and momentum variable. Thus it is sufficient to restrict the discussion to one unit cell $(x, p) \in [0, 2\pi] \times [0, 2\pi]$. Depending on the values of the parameters ϵ and k we find at least three but not more then seven critical points of different types (minimum, maximum and saddle point) per unit cell. To discuss these cases we have decomposed the parameter space $(\epsilon, k) \in \mathbf{R}^+ \times (0, 1]$ into five regions A to E as shown in Fig. 4.

In the Table 5 we list the critical points of $H(x, p)$ for each of these regions.

where $n, m \in \mathbf{Z}$ and $t \in [0, 2\pi]$. "a. max" and "a. min" denote an absolut maximum and an absolut minimum repectively, while "l. max" denotes a local maximum appearing in region A. In region C the cases Ib, II and IV coincide.

In Fig. 5 we have plotted the classical energy contours for typical parameter values of each region.

In all regions A to E we have a single absolute maximum at $(x, p) = (0, 0)$. In a vicinity around this point the Hamiltonian is parabolic and the system has solutions oscillating around the fixed point. The classical contours in phase space are compact.This allows to apply the usual semi classical Bohr-Sommerfeld quantisation as it has been introduced for the square lattice [26]. We will come back to this point in Section 7.

Except for the region C we also have a single absolut minimum in each unit cell. Locally near this point the Hamiltonian is again parabolic and we can apply the same type of semi-classical expansion as denoted above.

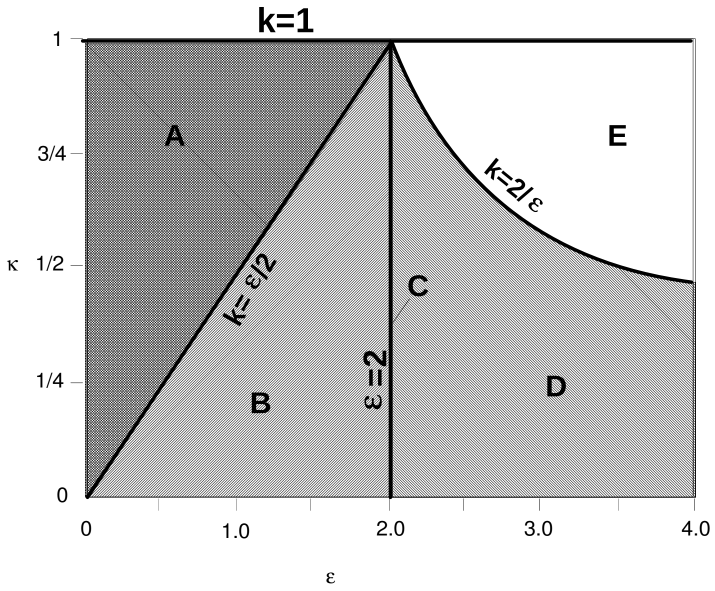

Figure 4: Regions A to E for critical points in parameter space

	critical point	energy	region				
	x,p		A	B	C	D	E
Ia)	$2\pi n$, $2\pi m$	$2(2\epsilon + k + \frac{1}{k})$	a. max.	a. max.	a. max.	a. max.	a. max.
Ib)	$2\pi n$, $\pi(2m+1)$ or $\pi(2n+1)$, $2\pi m$	$-2(k + \frac{1}{k})$	a. min.	a. min.	a. min=IV	saddle	saddle
Ic)	$\pi(2n+1)$, $\pi(2m+1)$	$2(-2\epsilon + k + \frac{1}{k})$	l. max.	saddle	saddle	saddle	a. min.
II	$\pi n \pm \arccos((-1)^{n+1}\frac{\epsilon k}{2})$, $\pi n \mp \arccos((-1)^{n+1}\frac{\epsilon k}{2})$	$2\left(\left(1-\frac{\epsilon^2}{2}\right)k - \frac{1}{k}\right)$	saddle	saddle	a. min= IV	a. min.	—
III	$\pi n \pm \arccos((-1)^{n+1}\frac{\epsilon}{2k})$, $-\pi n \pm \arccos((-1)^{n+1}\frac{\epsilon}{2k})$	$2\left(-k + \left(1-\frac{\epsilon^2}{2}\right)\frac{1}{k}\right)$	saddle	—	—	—	—
IV	$t \pm \arccos\left(-\frac{\epsilon k}{2}\cos(t)\right)$, $-t \pm \arccos\left(-\frac{\epsilon k}{2}\cos(t)\right)$	$-2(k + \frac{1}{k})$	—	—	a. min.	—	—

Table 2: Critical points of the classical symbol for the Quantum Pendulum

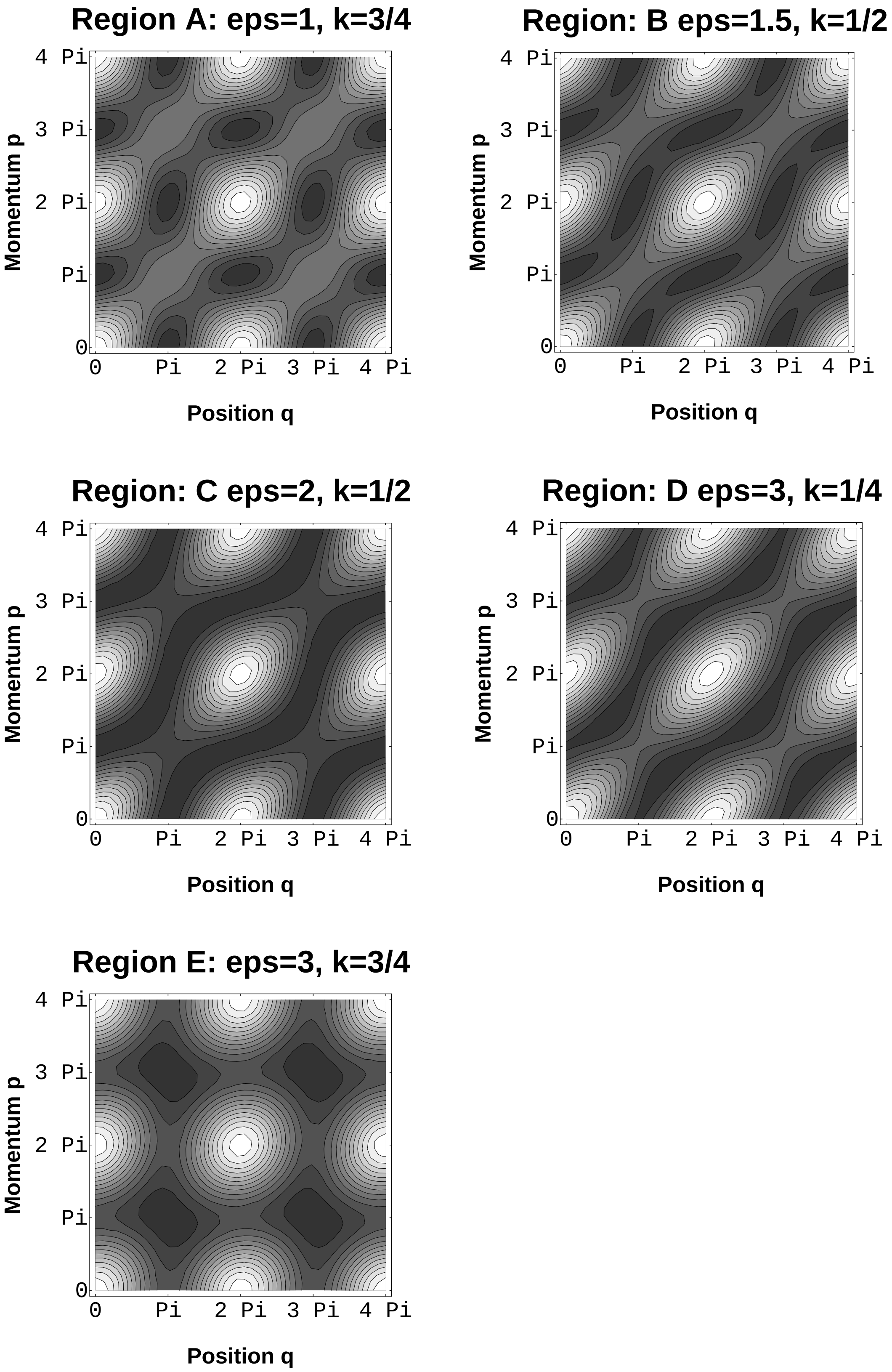

Region A: eps=1, k=3/4

Region: B eps=1.5, k=1/2

Region: C eps=2, k=1/2

Region: D eps=3, k=1/4

Region E: eps=3, k=3/4

Figure 5: Examples for classical contour levels in regions A to E

If the system has exactly one saddle point as in region E we have at the saddle point energy a separatrix level decomposing the phase space into two components containing the oscillating solutions of the minimum and maximum respectively. The contour at the separatrix level is not compact. This contour resembles the separatrix level in the triangular lattice [5] and square lattice (the later for $k = 1$) [26].

In regions A,B and D we have more than one saddle point per unit cell. In the energy range between the saddle point energies we observe rotating solutions of the classical system. Note that the classically rotating solutions fill an area of non-zero measure in phase space. This distinguishes the situation from the former case. It gives rise to an interesting semi classical behavior for this energies as will be seen in Section 7.

In region C, that is for $\epsilon = 2$, we have a degenerate situation where the absolute minumum and the lower saddle point coincide. The energy attains its minimum for a rotating solution. This is the "best" pendulum behavior we can expect for a bounded Hamiltonian.

In the system studied here we have rotating solutions for low energies and oscillating behavior at high energies. Since H is bounded from above and below we can also consider $-H$ which shows oscillation for low energies and rotation at high energies, as it is expected for a physical pendulum.

6 Spectrum of the discrete Quantum Pendulum

We have computed numerically the band spectrum of the discrete Quantum Pendulum for rational fluxes $\Phi = 2\pi\frac{p}{q}$ by diagonalizing the $q \times q$-matrix $H(\theta)$ at the critical points of the offset function $h(\theta)$. Using the scaling relation between the classical symbol and the offset function found in Section 4 we get the critical points from Table 5.

They are at $(0,0)$, $(0,\frac{\pi}{q})$ and $(\frac{\pi}{q},\frac{\pi}{q})$ for all ϵ and k.
At $(\pi/q + \arccos(-P(-\epsilon/2)(-1)^p k^q)/q, \pi/q - \arccos(-P(-\epsilon/2)(-1)^p k^q)/q)$ and $(\pi/q + \arccos(-P(-\epsilon/2)(-1)^p k^{-q})/q, \pi/q + \arccos(-P(-\epsilon/2)(-1)^p k^{-q})/q)$ we find critical points only if the argument of arccos is in the range $[-1,1]$. To compute the spectrum for fixed ϵ and k we diagonalize the matrix $H(\theta)$ for all critial points. The energies, up to five, thus obtained for each band where sorted and their minimal and maximal values give the lower and upper band edge, respectively.

In Fig. 6,7, 8, 9 and 10 we present typical spectra for the regions A to E. The pictures contain values of the flux $\Phi = 2\pi\frac{p}{q}$ for all relative prime integers $p, q \in \mathbf{Z}$ with $q \leq 40$. On the horizontal axis we draw the energy, while on the verical axis we raw the magnetic flux Φ in the range $[0, 2\pi] \approx [0, 6.28]$. A horizontal line in the picture is a spectral band of the Quantum Pendulum at the flux denoted on the vertical axis.

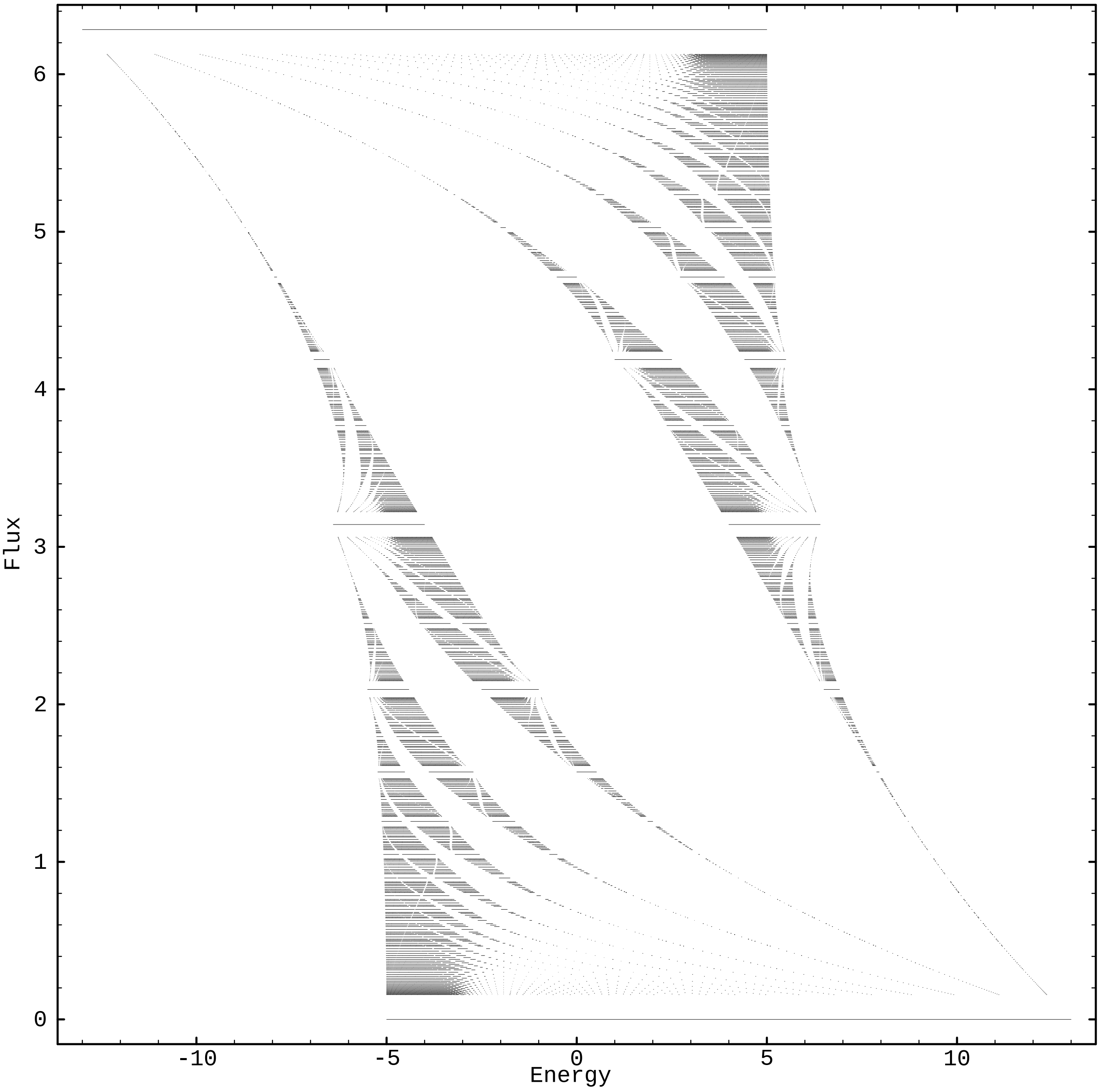

Figure 6: Spectrum of discrete Quantum Pendulum at $\epsilon = 1$ and $k = 3/4$ (region A)

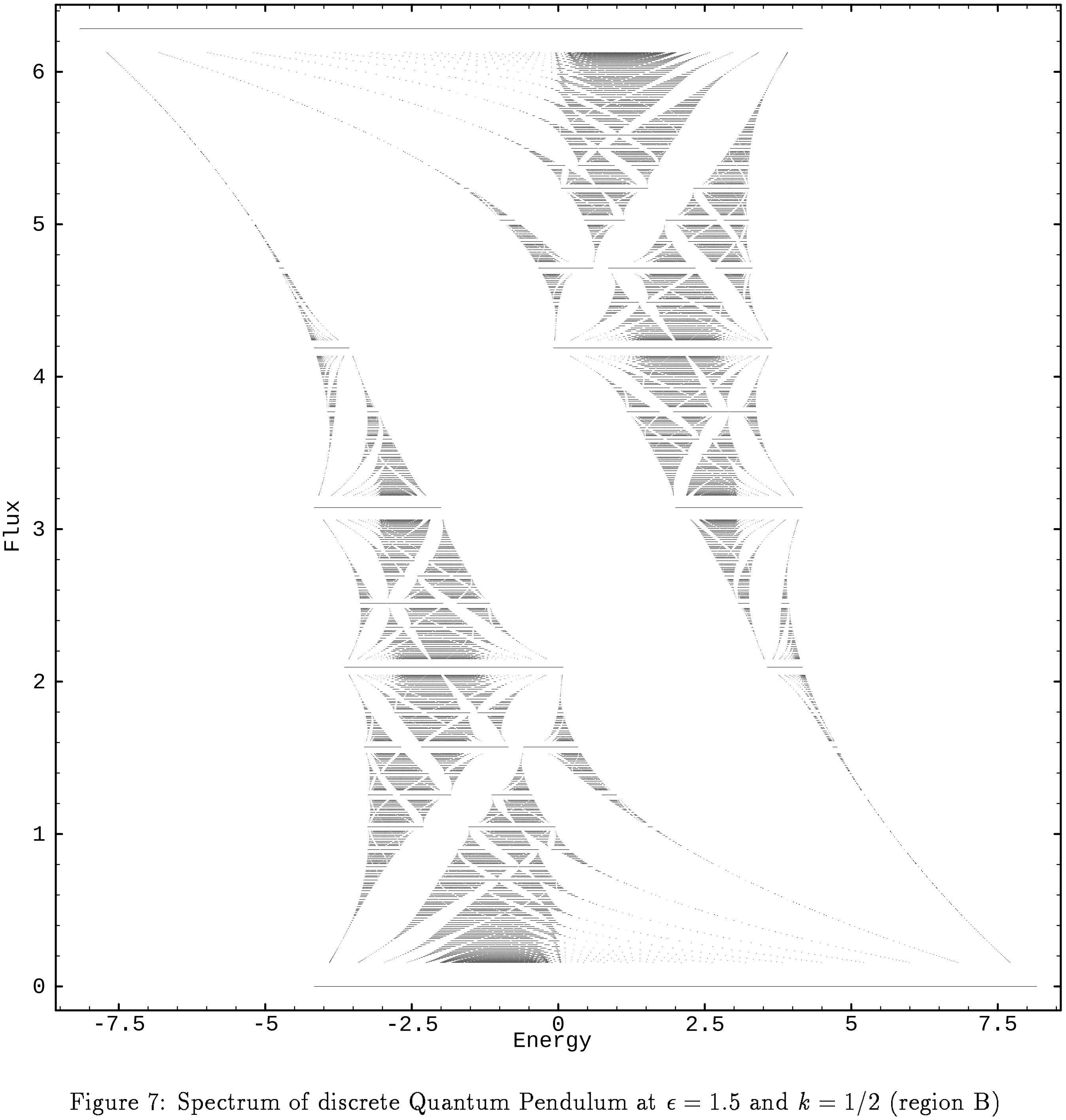

Figure 7: Spectrum of discrete Quantum Pendulum at $\epsilon = 1.5$ and $k = 1/2$ (region B)

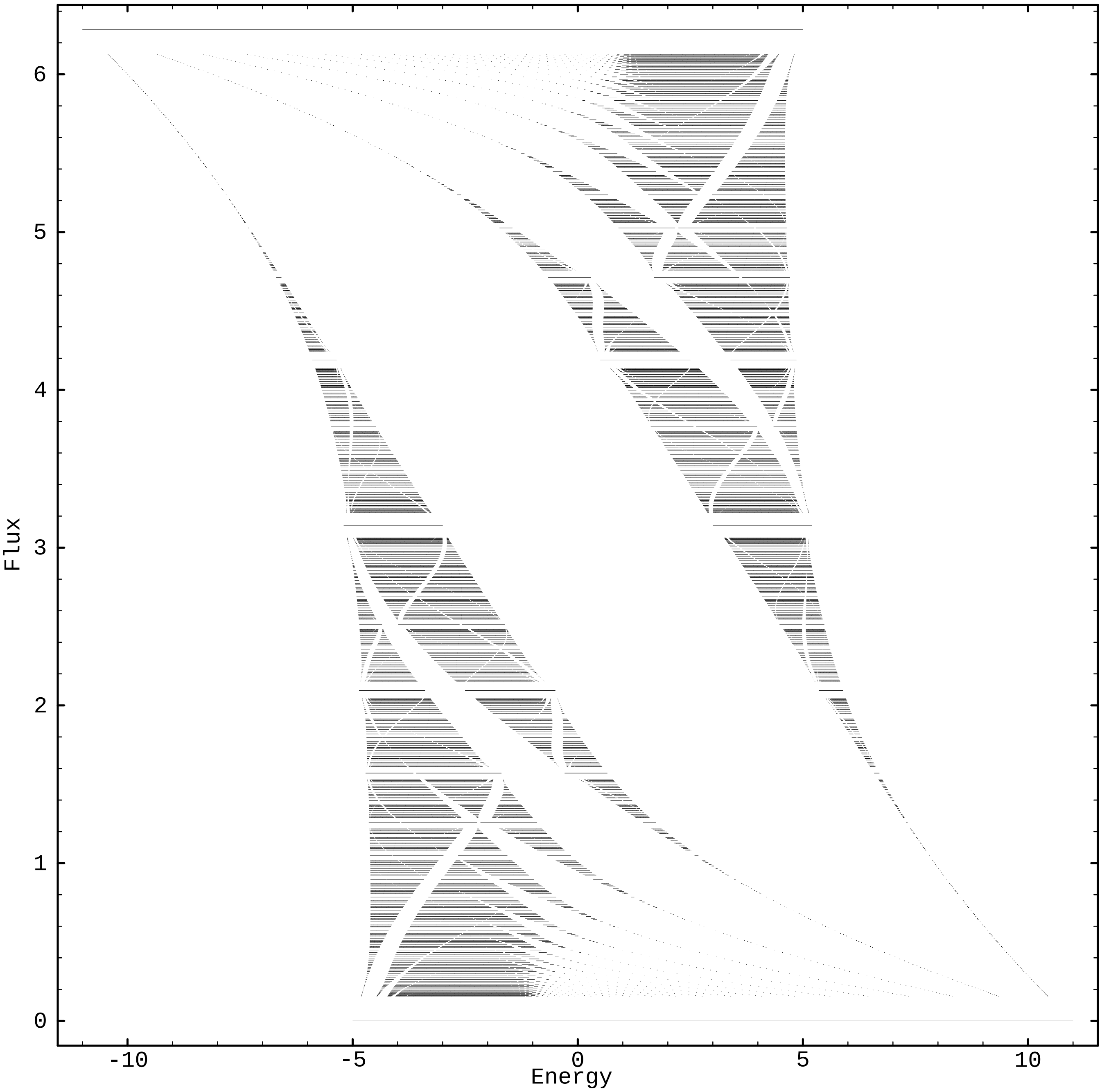

Figure 8: Spectrum of discrete Quantum Pendulum at $\epsilon = 2$ and $k = 1/2$ (region C)

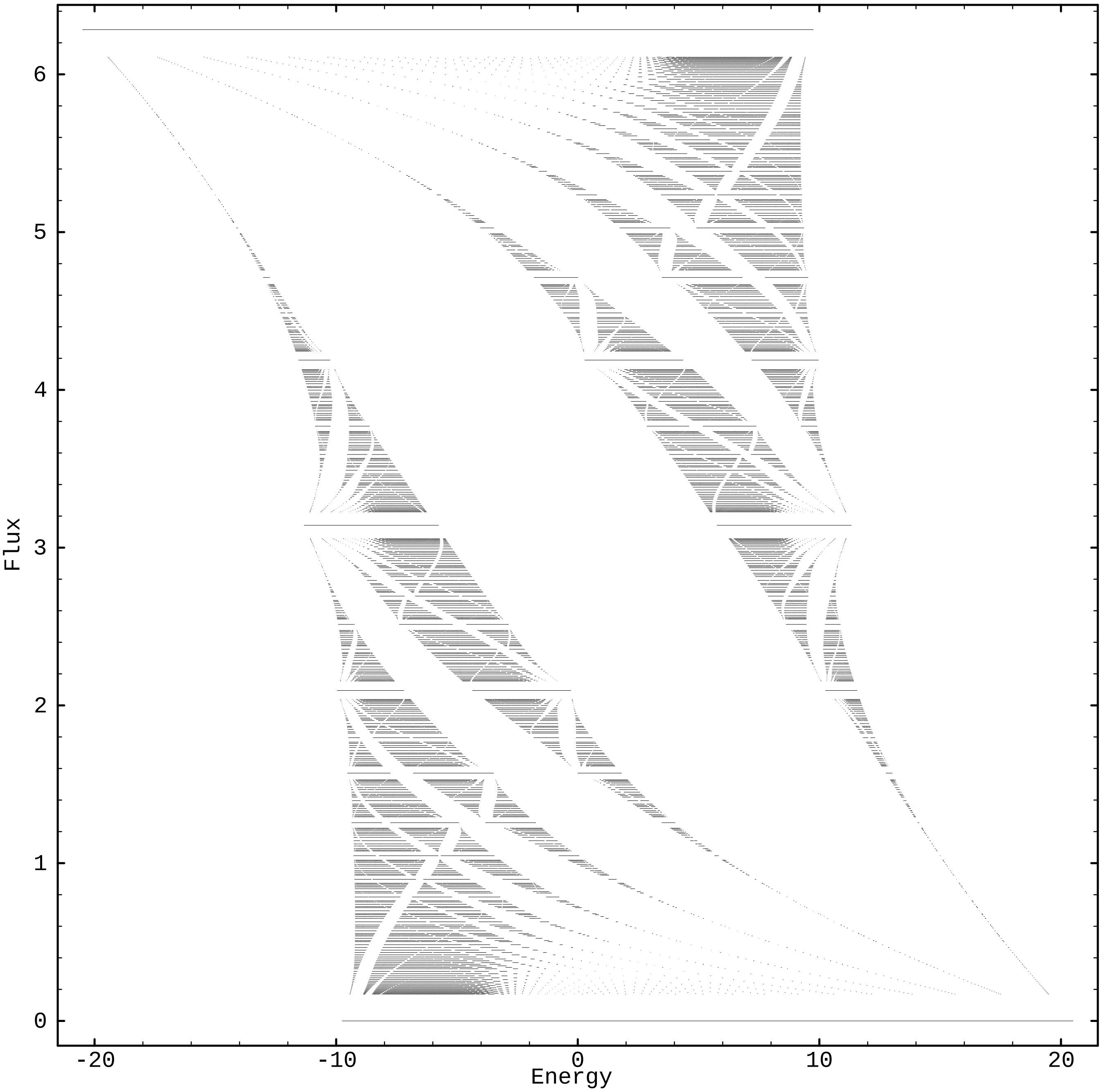
Flux
0
1
2
3
4
5
6
-20
-10
0
10
20
Energy